

# 利用激光腔内共振衰减技术研究 CH<sub>2</sub>CHO 自由基的近紫外吸收光谱\*

王黎明, 张劲松\*\*

(美国加州大学河滨分校化学系, 加州河滨市, 92521)

**摘要:** 利用激光腔内共振衰减技术(CRDS)获取了 CH<sub>2</sub>CHO 自由基的近紫外吸收光谱. 在此吸收光谱中, 有一从 28786 cm<sup>-1</sup> 起始的振动-电子带, 和一随能量而增加的宽吸收背景. 此 CRDS 吸收光谱和以前的低分辨率吸收光谱相一致, 其振动-电子吸收峰位置和激光诱导荧光光谱及光解产物谱中的峰位置相吻合.

**关键词:** 利用激光腔内共振衰减技术; CH<sub>2</sub>CHO 自由基; 近紫外吸收光谱

中图分类号: O64 文献标识码: A

## Near-Ultraviolet Absorption Spectrum of Vinoxy Radical ( CH<sub>2</sub>CHO ) by Cavity Ringdown Spectroscopy\*

Wang Liming, Zhang Jingsong\*\*

(Department of Chemistry, University of California, Riverside, CA 92521, U. S. A.)

**Abstract** Near-ultraviolet absorption spectrum of the  $\tilde{B}^2A'' \leftarrow \tilde{X}^2A''$  band of the vinoxy radical (CH<sub>2</sub>CHO) is recorded by cavity ringdown spectroscopy (CRDS). The absorption spectrum shows a series of vibronic bands starting from 28786 cm<sup>-1</sup> and an increasing broad background towards higher photon energy. The CRDS absorption spectrum is similar to an early low-resolution absorption spectrum; and the vibronic peak positions match well with those in the laser-induced fluorescence and photofragment yield spectra.

**Keywords** Cavity ringdown spectroscopy, Vinoxy radical, Near-Ultraviolet absorption spectrum

### 1 Introduction

Vinoxy radical (CH<sub>2</sub>CHO) is a prototypical alkenoxy radical important in combustion and atmospheric chemistry. Its formation has been observed in the reactions of O(<sup>3</sup>P) and OH radical with terminal olefins and olefinic radicals (for examples, O(<sup>3</sup>P) + C<sub>2</sub>H<sub>4</sub>,

OH + C<sub>2</sub>H<sub>2</sub>, and O(<sup>3</sup>P) + C<sub>2</sub>H<sub>3</sub>)<sup>[1-7]</sup>. Recently, CH<sub>2</sub>CHO has also been observed in the ozonolysis reaction of 2-butene under the minimized O<sub>2</sub> concentration condition, where the radical was formed from isomerization and dissociation of the Criegee intermediate CH<sub>3</sub>CHOO → CH<sub>2</sub>CHOOH → CH<sub>2</sub>CHO + OH<sup>[8]</sup>.

Spectroscopy and photodissociation of the vinoxy

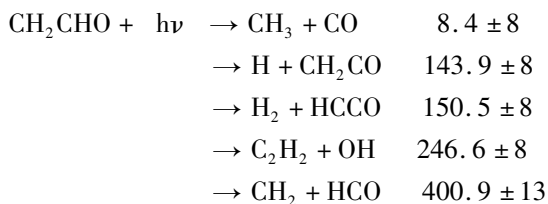
\* Project supported by the U. S. National Science Foundation (CHE-0111635) and the Alfred P. Sloan Foundation.

\*\* Corresponding author, Fax: 909-787-4713; E-mail: jingsong.zhang@ucr.edu; also at Air Pollution Research Center, University of California, Riverside, CA 92521. Received 31 May 2004.

radical have received extensive experimental and theoretical attention. The first absorption spectrum of the vinoxy radical was recorded by Ramsay<sup>[9]</sup>. A subsequent study by Hunziker *et al.*<sup>[10]</sup> discovered two absorption bands at low spectroscopic resolution: a near infrared (near-IR) band in the region of 8000 ~ 10000 cm<sup>-1</sup> due to the electronic transition  $\hat{A}^2A' \leftarrow \hat{X}^2A''$ , and a near ultraviolet (near-UV) band due to the  $\bar{B}^2A'' \leftarrow \hat{X}^2A''$  transition from the origin 28786 to 35700 cm<sup>-1</sup>. Recently, Zhu *et al.* reported a near-UV cavity ringdown absorption spectrum of vinoxy<sup>[11]</sup>, but only in the region of the  $\bar{B}^2A'' \leftarrow \hat{X}^2A''$  band origin. The near-UV absorption spectrum of vinoxy has several vibronic bands starting from the band origin at 28786 cm<sup>-1</sup>, and it becomes highly congested in the shorter wavelength region. The spectroscopy of the  $\bar{B}^2A''$  state has been extensively studied by laser-induced fluorescence (LIF)<sup>[12-14]</sup> with high resolution. The fluorescence intensity starts to deplete appreciably at about 1400 cm<sup>-1</sup> above the band origin; this is due to the nonradiative processes, such as avoided crossing and conical intersections, and the  $\bar{B}^2A''$  state decays via the internal conversion to the lower electronic states<sup>[15,16]</sup>. The nonradiative decay of the  $\bar{B}^2A''$  state eventually leads to fragmentation of the vinoxy radical, mainly to the CH<sub>3</sub> + CO and H + CH<sub>2</sub>CO product channels, with a branching ratio of approximately 1 to 4<sup>[17]</sup>. Both the LIF and the photofragment yield (PFY) spectrum reflect the absorption spectrum of vinoxy. While the fluorescence process is more important near the  $\bar{B}^2A'' \leftarrow \hat{X}^2A''$  band origin, the PFY increases significantly at higher photon energies.

Upon photoexcitation, the vinoxy radical has several dissociation channels<sup>[17]</sup>:

$$\Delta H_0^0 / (\text{kJ/mol})$$



The low dissociation thresholds, which suggest fast (pre)dissociation of the excited states, complicate the spectroscopic studies.

In this work, we have recorded the near-UV absorption spectrum of the vinoxy  $\bar{B}^2A'' \leftarrow \hat{X}^2A''$  band using cavity ringdown spectroscopy (CRDS). CRDS is a highly sensitive direct absorption technique; it is based on measurements of the rate (instead of the magnitude) of absorption of the laser light injected into a highly reflective optical cavity that contains the sample<sup>[18-20]</sup>. CRDS can provide a long effective absorption path (~ km) and thus high detection sensitivity. As CRDS is based on simple absorption, it is not complicated by fluorescence lifetime and intensity depletion due to the nonradiative processes of the excited electronic states. Thus CRDS is particularly useful for studying spectroscopy and chemical kinetics of transient free radicals<sup>[11,21]</sup>.

## 2 Experimental

The absorption spectrum was taken using CRDS<sup>[11,18-21]</sup>. The experimental setup has been described before in details<sup>[22]</sup>, and is briefly described here. The ringdown cavity was composed of a quartz tube (O. D. 25 mm) and two attached end chambers that housed the two high-reflectivity end mirrors (Los Gatos Research and Research Electro-Optics,  $R > 99.9\%$ ). The total cavity length  $L$  was 108 cm (from mirror to mirror). Inert gas such as nitrogen flowed in front of the mirrors across the end chambers to protect the mirrors from reactive gaseous species. Ethyl vinyl ether (EVE, CH<sub>2</sub>CHOCH<sub>2</sub>CH<sub>3</sub>) was used as the precursor of the vinoxy radical; it was kept at -45°C and its vapor was mixed with 101 kPa nitrogen carrier gas and entered and exited the cavity chamber near the center. Another nitrogen gas flow entered the cavity from one end and flowed out at the other, which further diluted the EVE gas mixture by a factor of 5 ~ 10. The gas mixture in the cavity chamber was maintained at room temperature and at 101 kPa pressure. The vinoxy radical was generated from 193 nm photolysis of EVE. The photolysis laser radiation was perpendicular to the quartz tube and was introduced near the center of the chamber, and the single-pass absorption path length  $l_s$  of the free radicals was about 5 cm. Near-UV CRDS probe laser radiation (1 ~ 2 mJ/pulse) was generated

from frequency doubling the output of a Nd : YAG 532 nm pumped dye laser ( Lambda Physik Scanmate II ). The laser linewidth was  $\sim 0.1 \sim 0.2 \text{ cm}^{-1}$ .

The small amount of laser radiation exiting the end of the cavity was detected by a photomultiplier tube ( PMT , EMI 9558 QB ). The signal from the PMT was collected by a digital storage oscilloscope ( Tektronix , TDS 3032 ) and was fitted as a single exponential decay curve

$$y(t) = a + be^{-t/\tau}$$

The decay rate ,  $1/\tau$  , is determined by the mirror transmission loss and sample absorption<sup>[11, 18-21]</sup> :

$$\frac{1}{\tau} = \frac{c}{L} [(1 - R) + \alpha l_s]$$

where  $\tau$  is the ringdown time ,  $L$  is the cavity length ,  $c$  is the speed of light ,  $R$  is the mirror reflectivity , and  $\alpha l_s$  is the single-pass absorbance of the sample (  $\alpha$  : the absorption coefficient ,  $l_s$  : the single-pass absorption length ). For the cavity filled with the gas mixture but without the absorbing radicals ( i. e. , with 193 nm photolysis laser off ) , the decay rate is

$$\frac{1}{\tau_0} = \frac{c}{L} (1 - R)$$

The  $1/\tau_0$  gives a broad and smooth baseline decay rate , as the mirror loss varies slowly with wavelength.

The absorbance of the sample per pass is

$$\alpha l_s = \frac{L}{c} \left( \frac{1}{\tau} - \frac{1}{\tau_0} \right)$$

The plot of absorbance , obtained as  $\frac{L}{c} \left( \frac{1}{\tau} - \frac{1}{\tau_0} \right)$  , as a function of laser wavelength yields the CRDS absorption spectrum of the free radical. The CRDS probe laser was typically scanned with 16 averages/step and 0.02 nm/step. The overall CRDS absorption spectrum of the vinyoxy radical was combined from the scans in different spectral regions , with their relative intensities properly normalized.

### 3 Results and discussions

The near-UV CRDS absorption spectrum of the vinyoxy  $\tilde{B}^2A'' \leftarrow \tilde{X}^2A''$  transition is shown in Fig. 1. This CRDS absorption spectrum was taken at 10  $\mu\text{s}$  delay between the 193 nm photolysis and the CRDS probe laser radiations. The rotational temperature of the vi-

noxy radical produced from the photolysis should have been relaxed to 300 K by collisions with the buffer gas at 101 kPa pressure , while there are still a few vibrational hot bands in the spectrum. The CRDS absorption spectrum is similar to the early absorption spectrum at low resolution by Hunziker *et al.*<sup>[10]</sup> , with the vibronic bands starting at 28786  $\text{cm}^{-1}$  and extended to above 33000  $\text{cm}^{-1}$  on top of a broad background feature. The CRDS absorption spectrum , however , reveals more details and peaks than the early absorption spectrum. The peak positions in the CRDS spectrum agree well with those in the LIF spectrum<sup>[12-14]</sup> and in the PFY spectrum ( predominantly due to the CH<sub>3</sub> + CO channel ) from fast-beam photodissociation by Osborn *et al.*<sup>[17]</sup>. As the CRDS spectrum is taken at room temperature , it is more congested than the LIF and PFY spectra with rotational temperatures of less than 30 K in the free jet<sup>[12-14, 17]</sup>. The spectral assignments of the prominent vibronic peaks are according to the theoretical Franck-Condon analysis by Yamaguchi *et al.*<sup>[23]</sup> and the PFY spectrum of Osborn *et al.*<sup>[17]</sup> , and are shown in Fig. 1. The sharp peaks represent the band-heads of the rotational profiles in the R-branch of the vibronic transitions. Despite the broad rotational profiles , this high-resolution CRDS absorption spectrum supports most of the early MCSCF calculations and the calculated Franck-Condon factors<sup>[23]</sup>. The vibrational modes of the vinyoxy  $\tilde{B}^2A''$  state that are excited in the  $\tilde{B}^2A'' \leftarrow \tilde{X}^2A''$  transition include  $\nu_4$  ( CO stretch ) ,  $\nu_5$  ( CHH scissors ) ,  $\nu_6$  ( OCH bend ) ,  $\nu_7$  ( CHH rock ) ,  $\nu_8$  ( CC stretch ) , and  $\nu_9$  ( CCO bend ). Excitations of these modes and their combinations are consistent with the geometric changes ( such as elongation of the C - C - O skeleton ) involved in the  $\tilde{B}^2A'' \leftarrow \tilde{X}^2A''$  transition<sup>[10, 12, 14, 17, 23]</sup>.

The profile of the entire CRDS absorption spectrum is different from those of the LIF and PFY spectra<sup>[14, 17, 23]</sup>. The origin transition  $0_0^0$  is the strongest line in the LIF spectrum , but the weakest in the PFY spectrum. The intensity in the LIF spectrum is greatly reduced above 1400  $\text{cm}^{-1}$  of the origin band  $0_0^0$  due to the nonradiative processes ; while the intensity in the PFY spectrum increases due to the correspondingly en-

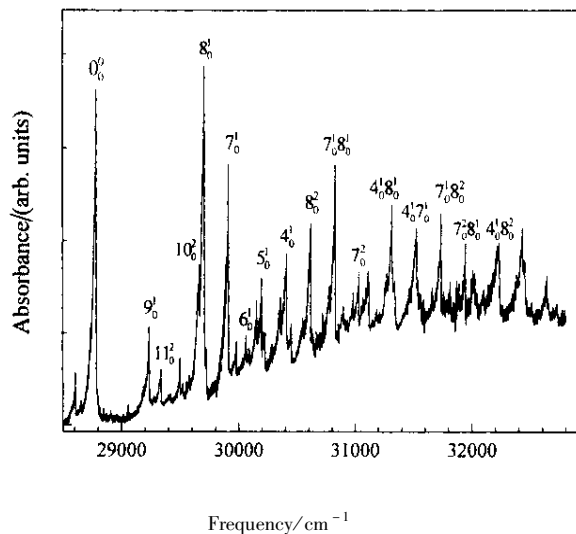


Fig. 1 CRDS absorption spectrum of the  $\tilde{B}^2A'' \leftarrow \tilde{X}^2A''$  band of the vinyloxy radical in the region of 28786 to 33000  $\text{cm}^{-1}$

hanced dissociation. The LIF and PFY spectra clearly demonstrate the competition between fluorescence and dissociation following the excitation to the  $\tilde{B}^2A''$  state. The CRDS absorption spectrum shows a series of vibronic bands which match well with those in the LIF and PFY spectra, and in addition, a broad background feature that increases with photon energy. To confirm that the broad feature in the CRDS absorption spectrum is due to the vinyloxy radical, the photolysis-probe time delay profiles of several vibronic peaks and the broad background are examined. Fig. 2 shows the comparison of a vibronic peak and the nearby broad background region. The time profiles of both features are essentially the same, suggesting that the broad background is also associated with the vinyloxy radical. The possible reasons for the broadened peaks and background of the  $\tilde{B}^2A''$  band in the CRDS absorption spectrum include: the difference in rotational temperature as mentioned above, unresolved vibronic bands, and fast nonradiative decay to the lower states. A rough estimation of density of vibrational levels of the  $\tilde{B}^2A''$  state is shown in Fig. 3, using the vibrational frequencies evaluated at the CASSCF(3,3) level<sup>[17]</sup>. With the increase of the vibrational energy in  $\tilde{B}^2A''$ , the number of the available vibrational states increases drastically. This could contribute a continuous broad background absorption towards shorter wavelength de-

spite the limitation from the Franck-Condon factors.

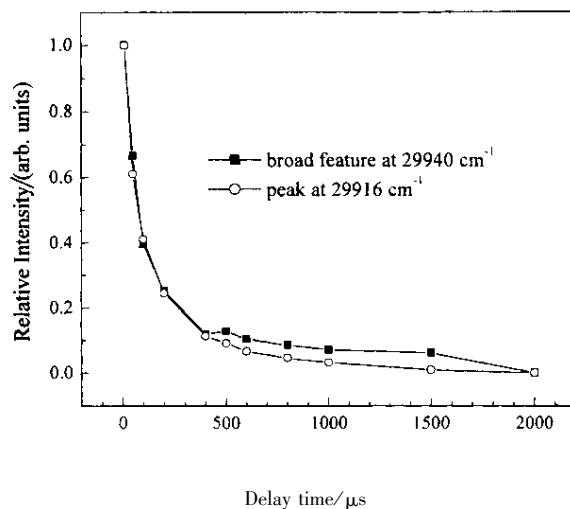


Fig. 2 Comparison of relative intensities of a vibronic peak (at 29916  $\text{cm}^{-1}$ ) and the broad absorption feature (at 29940  $\text{cm}^{-1}$ )

The maximum of each curve is normalized to unit. The delay time is between the 193 nm photolysis laser and the CRDS probe laser.

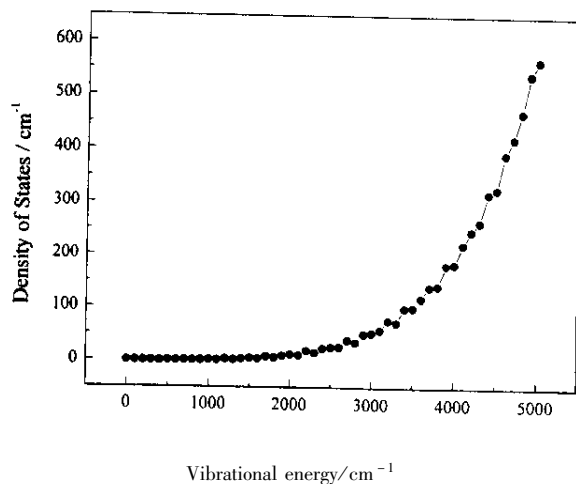


Fig. 3 Estimated density of states of the  $\tilde{B}^2A''$  state versus the available vibrational energy (relative to the ground vibrational level of the  $\tilde{B}^2A''$  state)

## References

- [1] Schmoltner A M, Chu P M, Brudzynski R J, Lee Y T. *J. Chem. Phys.*, 1989, **91**: 6926
- [2] Koda S, Endo Y, Tsuchiya S, Hirota E. *J. Phys. Chem.*, 1991, **95**: 1241
- [3] Abou-Zied K A, McDonald J D. *J. Chem. Phys.*, 1998, **109**: 1293

- [ 4 ] Morton M L , Szpunar D E , Butler L J. *J. Chem. Phys.* , 2001 , **115** : 204
- [ 5 ] Su H , Bersohn R. *J. Phys. Chem. A* , 2001 , **105** : 9178
- [ 6 ] Donaldson D J , Okuda I V , Sloan J J. *Chem. Phys. Lett.* , 1995 , **193** : 37
- [ 7 ] Schmidt V , Zhu G Y , Becjker K H , Fink E H. *Ber. Bunsen-Ges. Phys. Chem.* , 1985 , **89** : 321
- [ 8 ] Wang L. Ph. D. Thesis , University of California , Riverside , 2002.
- [ 9 ] Ramsay D A. *J. Chem. Phys.* , 1965 , **43** : S18
- [ 10 ] Hunziker H E , Knepe H , Wendt H R. *J. Photochem.* , 1981 , **17** : 377
- [ 11 ] Zhu L , Johnston G. *J. Phys. Chem.* , 1995 , **99** : 15114
- [ 12 ] DiMauro L F , Heaven M , Miller T A. *J. Chem. Phys.* , 1984 , **81** : 2339
- [ 13 ] Wan R , Chen X , Wu F , Weiner B R. *Chem. Phys. Lett.* , 1966 , **260** : 539
- [ 14 ] Brock L R , Rohlfing E A. *J. Chem. Phys.* , 1997 , **106** : 10048
- [ 15 ] Yamaguchi M. *Chem. Phys. Lett.* , 1994 , **221** : 531
- [ 16 ] Matsika S , Yarkony D R. *J. Chem. Phys.* , 2002 , **117** : 7198
- [ 17 ] Osborn D L , Choi H , Mordaunt D H , Bise R T , Neumark D M , Rohlfing C M. *J. Chem. Phys.* , 1997 , **106** : 3049
- [ 18 ] O'Keefe A , Deacon D A G. *Rev. Sci. Instrum.* , 1988 , **59** : 2544
- [ 19 ] Scherer J J , Paul J B , Okeefe A , Saykally R J. *Chem. Rev.* , 1997 , **97** : 25
- [ 20 ] Wheeler M D , Newman S M , OrrEwing A J , Ashfold M N R. *J. Chem. Soc. Faraday Trans.* , 1998 , **94** : 337
- [ 21 ] Yu T , Lin M C. *J. Am. Chem. Soc.* , 1993 , **115** : 4371
- [ 22 ] Wang L M , Zhang J S. *Environ. Sci. & Tech.* , 2000 , **34** : 4221
- [ 23 ] Yamaguchi M , Momose T , Shida T. *J. Chem. Phys.* , 1990 , **93** : 4211